

# Domain Structure and Functional Activity of the Recombinant Human Fibrinogen $\gamma$ -Module ( $\gamma$ 148–411)<sup>†</sup>

Leonid Medved,<sup>\*,‡</sup> Sergei Litvinovich,<sup>‡</sup> Tatiana Ugarova,<sup>§</sup> Yuri Matsuka,<sup>‡</sup> and Kenneth Ingham<sup>‡</sup>

J. Holland Laboratory, American Red Cross, Rockville, Maryland 20855, and Center for Thrombosis and Vascular Biology, Cleveland, Ohio 44195

Received November 11, 1996; Revised Manuscript Received January 16, 1997<sup>®</sup>

**ABSTRACT:** Human fibrinogen  $\gamma$ -module comprising residues  $\gamma$ 148–411 was expressed in *Escherichia coli* and refolded *in vitro*. Differential scanning calorimetry revealed that in addition to the two previously identified independently folded thermolabile domains, one in each half of the module, the  $\gamma$ -module also contains one or two thermostable domains that melt above 65 °C. To localize the latter, an NH<sub>2</sub>-terminal 6-kDa fragment was prepared by limited proteolysis of the recombinant  $\gamma$ -module. It melted at high temperature, indicating that this portion is folded into a compact structure that represents a thermostable domain, also identified in the proteolytic fibrinogen fragment D<sub>1</sub> which contains the natural  $\gamma$ -module. Thus the NH<sub>2</sub>-terminal half of the  $\gamma$ -module forms two domains, a thermostable one and a thermolabile one, leaving the rest of the module to be responsible for the formation of the other one or two domains. The thermal stability of some domains was lower in the recombinant  $\gamma$ -module than in its natural counterpart in D<sub>1</sub>, reflecting most probably the loss of interactions with neighboring domains; however, the major functional sites were essentially preserved. The module bound Ca<sup>2+</sup> and was stabilized by it against denaturation and proteolysis. It inhibited fibrin polymerization and was efficiently cross-linked by factor XIIIa. The  $\gamma$ -module supported adhesion of platelets via their GP IIb/IIIa ( $\alpha_{IIb}\beta_3$ ) receptor in the same manner as D<sub>1</sub> fragment. It also supported the adhesion of  $\alpha_M\beta_2$ - (Mac-1-) transfected cells and in the fluid phase was more effective than D<sub>1</sub> as an inhibitor of that adhesion, suggesting that the Mac-1 binding site is better exposed.

Fibrinogen is mainly known as a blood clotting protein that, after activation by thrombin, undergoes polymerization to prevent the loss of blood upon vascular injury. In addition, fibrinogen is involved in a number of important physiological and pathological processes including fibrinolysis, inflammation, angiogenesis, wound healing, and atherogenesis. Its polyfunctional character is connected with its multidomain structure and the presence of multiple interaction sites that allow its interaction with other proteins and cells.

Fibrinogen (340 kDa) consists of two identical disulfide-bonded subunits, each of which is formed by three nonidentical polypeptide chains, A $\alpha$ , B $\beta$ , and  $\gamma$  (Doolittle, 1984). These chains form at least 14 compact domains, seven in each subunit, whose borders and independent folding status were established by calorimetric analysis (Privalov & Medved, 1982; Medved *et al.*, 1983, 1986; Medved, 1990; Litvinovich *et al.*, 1995). It was demonstrated that the COOH-terminal region of each subunit corresponding to the proteolytic D<sub>1</sub> fragment (D region) contains at least five independently folded domains (Medved *et al.*, 1986). One is formed by the NH<sub>2</sub>-terminal portion of all three chains in a coiled-coil conformation (thermostable domain, TSD), while the COOH-terminal portions of the B $\beta$  and  $\gamma$  chains each form at least two thermolabile domains. These portions

(approximately 260 amino acid residues each) are homologous to each other and to a number of sequences found in other proteins, where they are referred to as the fibrinogen-like module (Doolittle, 1992). They are functionally important in fibrinogen since they contain a Ca<sup>2+</sup>-binding site and a number of interaction sites that are involved in fibrin assembly, plasminogen activation, platelet aggregation, and interaction with leukocytes and bacteria. Some of these sites were localized and partially characterized. In particular, the module formed by the 148–411 region of the  $\gamma$  chain ( $\gamma$ -module) contains a major polymerization site complementary to the Gly-Pro-Arg-containing site in the central region (Doolittle, 1994). Its exact location is still unknown. The Ca<sup>2+</sup>-binding site of the  $\gamma$ -module was proposed to be in the 4-kDa stretch starting at  $\gamma$ 303 (Nieuwenhuizen & Haverkate, 1983). The site that promotes activation of plasminogen by tPA was localized in  $\gamma$ 311–379 (Yonekawa *et al.*, 1992). The fibrinogen-dependent platelet aggregation process involves an interaction between integrin IIb/IIIa ( $\alpha_{IIb}\beta_3$ ) and a complementary site that was localized in the COOH-terminal 397–411 portion of the  $\gamma$ -module (Niewiarowski *et al.*, 1983). This portion also interacts with *Staphylococcus aureus* (Hawiger *et al.*, 1983) and contains reactive Gln398 and Lys406 residues that are cross-linked by factor XIIIa, resulting in  $\gamma$ – $\gamma$  dimer formation and stabilization of fibrin gels (Doolittle, 1994; Henschen & McDonagh, 1986). The NH<sub>2</sub>-terminal portion of the  $\gamma$ -module including residues 190–202 interacts with leukocyte integrin Mac-1 ( $\alpha_M\beta_2$ ) during the fibrinogen-dependent inflammatory response (Altieri *et al.*, 1993).

<sup>†</sup> Supported by National Institutes of Health Grant HL21791 and American Heart Association, Northeast Ohio Affiliate, 249-BJ.

\* To whom correspondence should be addressed at Holland Laboratory, 15601 Crabbs Branch Way, Rockville, MD 20855. Phone: (301) 738-0719. FAX: (301) 738-0794. e-mail: medvedl@usa.redcross.org.

<sup>‡</sup> American Red Cross.

<sup>§</sup> Center for Thrombosis and Vascular Biology.

<sup>®</sup> Abstract published in *Advance ACS Abstracts*, April 1, 1997.



solubilized in 4 M guanidine hydrochloride (GdnHCl).<sup>1</sup> The NH<sub>2</sub>-terminal sequence analysis at this stage was performed with a Hewlett-Packard Model G1000S sequenator and confirmed that the 30-kDa protein corresponds to the fibrinogen  $\gamma$ -module with more than 95% purity.

**Refolding** was accomplished by slow dialysis as follows. The protein in 4 M GdnHCl was 10-fold diluted with 10 M urea to a final concentration of 0.2–0.25 mg/mL and dialyzed against a 4-fold volume of 8 M urea at room temperature for several hours. Then the concentration of urea in the container was slowly reduced to 0.125 M by addition with a peristaltic pump of 20 mM Tris buffer, pH 8.0, at 4 °C over a period of 36 h followed by extensive dialysis of the protein versus the same buffer. Sometimes a slight pellet was observed that was removed by centrifugation. The protein was further dialyzed versus TBS (20 mM Tris buffer, pH 7.4, with 0.15 M NaCl) containing 1 mM Ca<sup>2+</sup>, resulting in the appearance of a large pellet. The latter was removed by centrifugation and the TBS-soluble protein was concentrated to 1.0–2.0 mg/mL with a Centrprep 10 concentrator (Amicon) and stored frozen at –20 °C.

**Preparations of Fragments.** Fibrinogen fragments, human D<sub>1</sub> and bovine D<sub>H</sub>, both containing the TSD domain plus  $\gamma$ - and  $\beta$ -modules, and bovine TSD were prepared by the procedures described earlier (Medved *et al.*, 1982; Litvinovich *et al.*, 1995; Cierniewski *et al.*, 1986). The P1 peptide (GWTVFQKRLDGSV), corresponding to  $\gamma$  chain residues 190–202, was synthesized by solid-phase technology using an Applied Biosystems Model 430 peptide synthesizer (Foster City, CA).

**Factor XIIIa-Mediated Cross-Linking.** The reaction was carried out in TBS containing 1 mM CaCl<sub>2</sub> at 25 °C. The cross-linking was initiated by addition of thrombin (Sigma) to a solution containing 40  $\mu$ g/mL recombinant factor XIII and 1.3 mg/mL  $\gamma$ -module or 3.6 mg/mL D<sub>1</sub> fragment. Recombinant factor XIII a<sub>2</sub> subunit was obtained from Dr. Paul Bishop of ZymoGenetics (Bishop *et al.*, 1990).

**Turbidity Measurement.** Polymerization of fibrin was initiated by dilution of concentrated monomeric fibrin (kept at acidic pH) with 20 mM Tris-HCl, pH 7.4, 0.15 M NaCl, and 1 mM CaCl<sub>2</sub> to a final concentration of 0.05 mg/mL at room temperature. Fibrin monomer was prepared by the procedures described earlier (Gorkun *et al.*, 1994). Turbidity changes upon polymerization were recorded on a Perkin-Elmer Lambda 5 spectrophotometer at 350 nm. The delay in turbidity onset (lag time) and the maximum rate of turbidity growth ( $V_{\max}$ ) were estimated from the turbidity curves as described earlier (Medved *et al.*, 1985).

**Cell Adhesion Assay.** Platelets and human kidney 293 cells expressing the wild-type recombinant  $\alpha_M\beta_2$  receptor were used to test the adhesive properties of the recombinant  $\gamma$ -module. Fresh aspirin-free human blood, anticoagulated with acid/citrate/dextrose and drawn into 2.8  $\mu$ M prostaglandin E<sub>1</sub>, was used to isolate platelets. The platelets were labeled with Na<sub>2</sub><sup>51</sup>CrO<sub>4</sub> (1 mCi for 30 min) in platelet-rich plasma and isolated by gel filtration on Sepharose 2B-CL in divalent cation-free Tyrode buffer, pH 7.2. Platelets were

resuspended at 10<sup>8</sup>/mL in Hanks' balanced salt solution (HBSS) supplemented with 1 mg/mL bovine serum albumin and 1 mM Ca<sup>2+</sup> and Mg<sup>2+</sup>.

The cells expressing wild-type  $\alpha_M\beta_2$  receptor were a generous gift from Dr. L. Zhang (Cleveland Clinic Foundation) and were prepared as described (Zhang & Plow, 1996). The cells were labeled with Na<sub>2</sub><sup>51</sup>CrO<sub>4</sub> (1 mCi for 1 h). After being washed, the cells were resuspended at 10<sup>6</sup>/mL in HBSS supplemented with 1 mg/mL BSA and 1 mM Ca<sup>2+</sup> and Mg<sup>2+</sup>. For adhesion assays, 10<sup>7</sup> platelets and 10<sup>5</sup>  $\alpha_M\beta_2$ -expressing cells were added in triplicate to individual wells of 48-well tissue culture plates (Costar, Cambridge, MA) coated with different concentrations of D<sub>1</sub> fragment or  $\gamma$ -module and postcoated with 1% heat-denatured bovine serum albumin for platelets and with 0.05% poly(vinylpyrrolidone) for  $\alpha_M\beta_2$ -expressing cells. In some experiments the cells were mixed with selected concentrations of competitor (D<sub>1</sub> fragment,  $\gamma$ -module, or peptide P1). After 15 min at 22 °C, the cells were added to individual wells of the plate coated with 10  $\mu$ g/mL (0.2 mL/well) of  $\gamma$ -module. Cells were allowed to adhere for 1 h at 37 °C in 5% CO<sub>2</sub> humidified atmosphere. The nonadherent cells were removed by three washes with 0.01 M phosphate buffer, pH 7.3, with 0.15 M NaCl. The adherent cells were solubilized with 2% SDS, and bound <sup>51</sup>Cr was quantitated in a  $\beta$  counter.

**Fluorescence measurements** of thermal unfolding were performed by monitoring either intrinsic fluorescence intensity at 370 nm or the ratio of the intensity at 370 nm to that at 330 nm with excitation at 280 nm in an SLM 8000-C fluorometer. Changes in these parameters provide a sensitive method for detecting denaturation transitions. However, these parameters are not directly proportional to the degree of unfolding, and the midpoint of the transition ( $T_m$ ) estimated in this manner may be less accurate than those obtained by other methods. Temperature was controlled with a circulating water bath programmed to raise the temperature at  $\approx$ 1 °C/min. Protein concentration was 0.04–0.05 mg/mL.

**Calorimetric Study.** Differential scanning calorimetry (DSC) measurements were made with a DASM-4M calorimeter (Privalov & Potekhin, 1986) in the temperature range 10–130 °C at a scan rate of 1 °C/min. Protein concentrations varied from 0.6 to 1.0 mg/mL. These were determined spectrophotometrically using extinction coefficients ( $E_{280,1\%}$ ) equal to 20.0 and 24.8 for D fragment and  $\gamma$ -module, respectively, and  $E_{275,1\%} = 8.0$  for TSD fragment. Those for D and TSD fragments were determined earlier (Privalov & Medved, 1982; Medved *et al.*, 1982), while that for  $\gamma$ -module was calculated from the amino acid composition (Edelhoch, 1967; Gill & von Hippel, 1989). The DSC curves were corrected for an instrumental baseline obtained by heating the solvent. Melting temperatures ( $T_m$ ) and the enthalpies of denaturation were determined from the DSC curves using software provided by Dr. V. Filimonov (Institute of Protein Research, Pouschino, Russia). Deconvolution analysis was performed according to Privalov and Potekhin (1986) and Filimonov *et al.* (1982) using the same software.

## RESULTS

**Preparation of the Recombinant Fibrinogen  $\gamma$ -Module.** The recombinant  $\gamma$ -module comprising residues Ile148–Val411 was directly produced in *E. coli* host cells using the pET-20b expression vector as described in Materials and

<sup>1</sup> Abbreviations:  $C_p$ , heat capacity;  $\Delta C_{p,exc}$ , excess heat capacity; DSC, differential scanning calorimetry; GdnHCl, guanidine hydrochloride; HBSS, Hanks' balanced salt solution; TBS, Tris-buffered saline (20 mM Tris buffer, pH 7.4, with 0.15 M NaCl);  $T_m$ , midpoint of the denaturation.

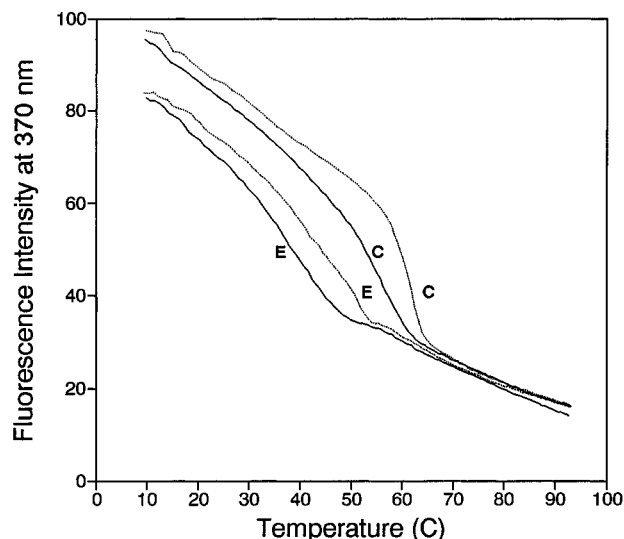


FIGURE 2: Fluorescence-detected thermal denaturation of the recombinant  $\gamma$ -module (solid curves) and human fibrinogen D<sub>1</sub> fragment (dotted curves). The experiments were performed in 100 mM Gly, pH 8.6, containing either 0.5 mM Ca<sup>2+</sup> (curves C) or 1 mM EDTA (curves E).

**Methods.** Since the  $\gamma$ -module was the major insoluble product of the cells (Figure 1, lane 2 in the gel), it was easily purified by repeated washing of the pellet (lanes 4–6) and then solubilized in 4 M GdnHCl at a yield of ~140 mg/L of bacterial culture. It was largely monomeric (lane 6) and failed to react with the sulfhydryl-specific probe pyrenyl-maleimide, indicating that its four cysteine residues form two intrachain disulfide bonds. To check if they are formed correctly, the  $\gamma$ -module was digested with cyanogen bromide as described earlier (Litvinovich *et al.*, 1995) and the digest was fractionated by HPLC. Sequence analysis of the individual fractions revealed the presence of the internally cleaved reducible fragment consisting of two portions starting at  $\gamma$ 311 and 337, as expected if the  $\gamma$ 326–339 disulfide is formed correctly (Figure 1, upper scheme), leaving another pair,  $\gamma$ 153–182, to form the other correct disulfide. This made it unnecessary to include redox reagents in the refolding protocol. The protein was refolded by slow dialysis from urea as described in Materials and Methods. In spite of the fact that all protein was soluble after the dialysis vs 20 mM Tris, pH 8.0, the majority was pelleted after subsequent dialysis versus TBS containing 1 mM Ca<sup>2+</sup>, reducing the final yield of the refolded protein to about 15–20% that produced by bacteria. When the pellet was recycled, i.e., dissolved in 10 M urea and subjected to slow dialysis by the same procedure, an additional portion of the refolded protein was prepared, increasing the total yield. SDS–PAGE of  $\gamma$ -module revealed a single band in both nonreducing and reducing conditions (lanes 7 and 8). Size-exclusion chromatography on Superdex 75 also revealed a single peak corresponding to the monomeric form (not shown).

**Fluorescence Study.** The refolded  $\gamma$ -module exhibited a fluorescence spectrum with  $\lambda_{\text{max}}$  at 343 nm consistent with the presence of a compact structure and similar to that of the human fibrinogen D<sub>1</sub> fragment that contains this module (not shown). When it was heated in the fluorometer while the fluorescence intensity was monitored at 370 nm, the  $\gamma$ -module produced a sigmoidal transition in the presence of Ca<sup>2+</sup> indicating heat-induced cooperative unfolding (Figure 2, solid curve C). In the presence of EDTA the transition

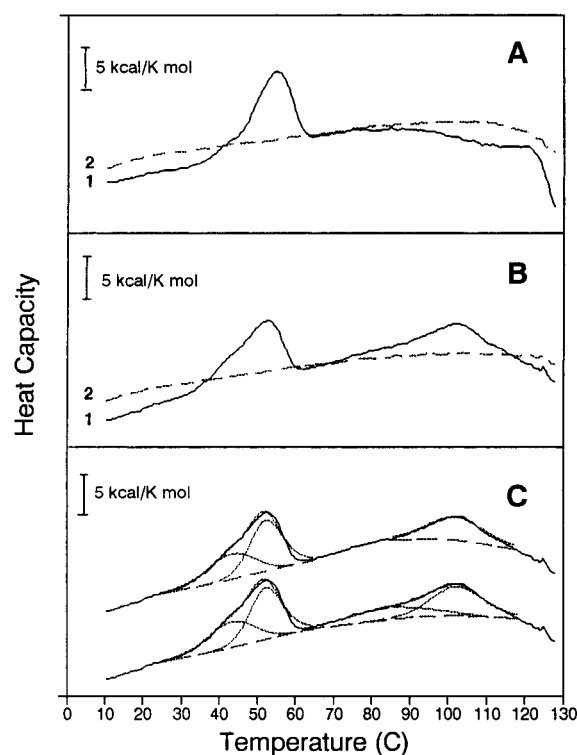


FIGURE 3: Differential scanning calorimetry curves of the recombinant  $\gamma$ -module (panels A and B) and the results of their deconvolution analysis (panel C). The curves in panels A and B were obtained in 20 mM Gly, pH 8.6, in the presence or absence of 0.5 mM Ca<sup>2+</sup>, respectively. First and second heatings are designated by solid curves 1 and broken curves 2, respectively. The curves in panel C represent the results of deconvolution analysis of the curve from panel B with alternatively selected baselines (see text). The broken lines in panel C indicate the manner in which the excess heat capacities were determined; the dotted lines represent the component two-state transitions, whose parameters are presented in Table 2, and the best fits obtained by deconvolution.

was shifted to lower temperature (solid curve E), reflecting the well-known thermal stabilization upon binding of calcium ions to the  $\gamma$  chain and indicating that the Ca<sup>2+</sup>-binding site in the recombinant  $\gamma$ -module is preserved. Similar experiments were performed with the D<sub>1</sub> fragment for comparison (Figure 2, dotted curves). The denaturation of the D<sub>1</sub> fragment was also Ca<sup>2+</sup>-dependent but occurred at higher temperature than that of the  $\gamma$ -module indicating that the latter is destabilized in comparison with its natural counterpart in D<sub>1</sub>.

**Calorimetric Study.** To examine the domain structure of the recombinant  $\gamma$ -module, we performed a study of its denaturation by differential scanning calorimetry. When heated in the calorimeter in the presence of Ca<sup>2+</sup>, recombinant  $\gamma$ -module exhibited an endotherm with a heat absorption peak at about 55 °C, followed by a downward turn in the heat capacity ( $C_p$ ) function at higher temperature (see typical example in Figure 3A, curve 1). The downward turn was connected most probably with aggregation of the denatured protein since solutions become turbid after heating up to 130 °C. This distorted the high-temperature portion of the endotherm, precluding its thermodynamic analysis. At the same time, removal of Ca<sup>2+</sup> prior to the experiment by extensive dialysis prevented aggregation and allowed one to observe, in addition to the lower temperature heat absorption peak that now occurs at 52 °C, a high-temperature one with  $T_m$  at about 100 °C (Figure 3B, curve 1). The latter

Table 2: Summary of Thermodynamic Parameters of the Melting Process of Recombinant  $\gamma$ -Module and Natural Proteolytic Fragments of Human ( $D_1$ ) and Bovine ( $D_H$  and TSD) Fibrinogen<sup>a</sup>

protein	pH	first peak			second peak			third peak		
		tr no.	$T_m$	$\Delta H$	tr no.	$T_m$	$\Delta H$	tr no.	$T_m$	$\Delta H$
$\gamma$ -module	8.6	1	43.0	47	1 <sup>b</sup>	102.1	55			
		2	52.2	69	1 <sup>b</sup>	84.5	37			
$D_1$ fragment	8.6	1	53.5	89	2 <sup>b</sup>	102.4	60			
		2	53.1	107	2	91.1	67			
		3	56.4	115						
		4	57.2	92						
$D_H$ fragment	8.0	1	54.9	82	1	90.0	56	1	119.9	86
		2	55.2	97	2	97.1	65			
		3	59.8	81						
		4	57.0	108						
TSD fragment	8.0							1	100.6	87

<sup>a</sup> Experiments were performed in 20 mM Gly buffer. The enthalpies of individual transitions ( $\Delta H$ ) are given in kilocalories per mole; transition temperatures ( $T_m$ ) are given in degrees Celsius. <sup>b</sup> Results of the deconvolution analysis determined with the different baselines shown in the upper and lower curves of Figure 3C (see text).

peak becomes more obvious when the endotherm is compared with that obtained upon second heating (broken curve 2), which represents the  $C_p$  function of the denatured protein. The lower temperature peak was fitted well by two two-state transitions (Figure 3C and Table 2), indicating the melting of two thermolabile domains. Similar results were obtained upon deconvolution of the corresponding peak obtained in the presence of  $Ca^{2+}$  (not shown). The deconvolution analysis of the high-temperature peak was less definite due to the difficulties in the proper selection of the baseline for determination of the area under the peak (excess heat capacity,  $\Delta C_{p,exc}$ ). Two extreme cases corresponding to the minimal and maximal area are shown in Figure 3C, upper and lower curves, respectively, where either one or two domains are inferred by deconvolution. In spite of the ambiguity it is clear that the recombinant  $\gamma$ -module contains, in addition to the expected two thermolabile domains, at least one thermostable domain that was not revealed in our previous experiments with the natural protein (Privalov & Medved, 1982; Medved *et al.*, 1986; Litvinovich *et al.*, 1995).

To test if similar thermostable domains are present in natural fibrinogen, we examined the denaturation of bovine fibrinogen  $D_H$  and its human analog  $D_1$ , each consisting of a TSD domain, a  $\gamma$ -module, and the homologous  $\beta$ -module. When melted in the calorimeter at pH 8.6, the same conditions as for the  $\gamma$ -module, human  $D_1$  exhibited a low-temperature transition with  $T_m$  at 56 °C and a higher temperature one with  $T_m$  at 88 °C, followed by a downward turn (Figure 4, curve 1). A similar curve was obtained with bovine  $D_H$  in the same conditions (not shown). At pH 8.0 the downward turn was less prominent in  $D_H$ , allowing the observation of a third peak that starts at about 110 °C (curve 2) and was probably masked by aggregation at higher pH in both bovine and human D fragments. The first peak in both human and bovine D fragments that occurred in approximately the same temperature range as the corresponding peak in recombinant  $\gamma$ -module was fitted by four transitions (Figure 4 and Table 2), reflecting the melting of four thermolabile domains. This is in good agreement with the presence of two thermolabile domains in the  $\gamma$ -module, as

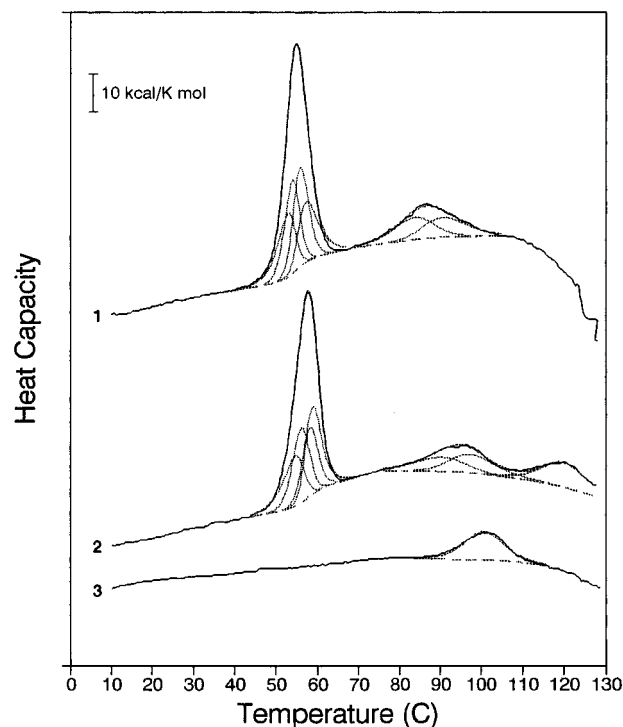


FIGURE 4: Differential scanning calorimetry curves of the human fibrinogen  $D_1$  fragment (curve 1) and bovine  $D_H$  and TSD fragments (curves 2 and 3, respectively). The experiments were performed in 20 mM Gly, pH 8.6 (curve 1) and 8.0 (curves 2 and 3). The broken lines indicate the manner in which the excess heat capacities were determined. The dotted lines represent the component two-state transitions, whose parameters are presented in Table 2, and the best fits obtained by deconvolution.

described above, and two in the  $\beta$ -module as reported earlier (Medved *et al.*, 1986). The second peak in both fragments was fitted by two transitions, reflecting the melting of two additional thermostable domains, probably one in each of the  $\beta$ - and  $\gamma$ -modules. The third peak was described well by a single transition and corresponds most probably to the melting of the TSD domain since the latter, when isolated by proteolysis, also melted in a single transition, albeit at a lower temperature (curve 3). It should be noted that the above analysis reveals the minimal number of domains since the denaturation process of D fragments may not be completed at 130 °C and one cannot exclude the presence of additional thermostable domain(s) that melt beyond the studied temperature range. Thus the results indicate that in addition to the previously identified thermostable domain (TSD), the natural D fragment contains at least two more thermostable domains, one in each of the  $\gamma$ - and  $\beta$ -modules, as first revealed here in the recombinant  $\gamma$ -module. This discovery became possible due to the use of a calorimeter which registers endotherms up to 130 °C (Privalov & Potekhin, 1986) and whose greater sensitivity allows the use of lower protein concentration, thereby reducing undesirable aggregation effects.

**Proteolytic Fragmentation of the  $\gamma$ -Module.** Digestion of the  $\gamma$ -module with chymotrypsin in the presence of EDTA resulted in the appearance of several discrete fragments (Figure 5A). The degradation was much slower in the presence of  $Ca^{2+}$ , indicating that calcium ions protect the  $\gamma$ -module against proteolysis as reported for natural fibrinogen and its  $D_1$  fragment (Nieuwenhuizen & Haverkate, 1983;

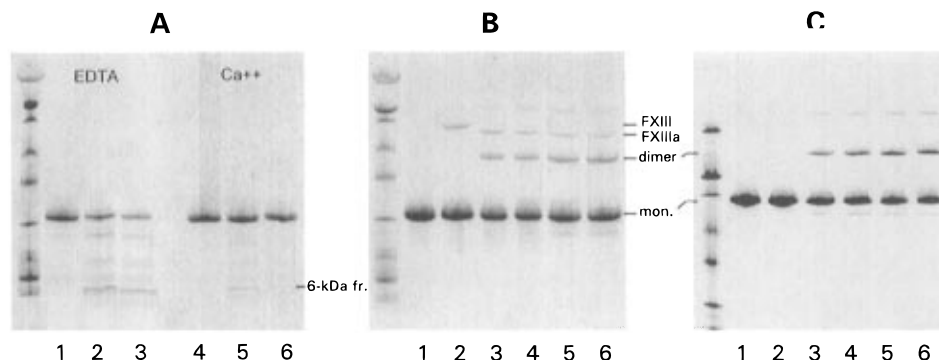


FIGURE 5: SDS-PAGE analysis of the time course of chymotryptic digestion of the recombinant  $\gamma$ -module (A) and factor XIIIa-catalyzed cross-linking of the recombinant  $\gamma$ -module (B) and fibrinogen fragment D<sub>1</sub> (C). Panel A represents the  $\gamma$ -module before (lanes 1 and 4) and 30 min (lanes 2 and 5) and 60 min (lanes 3 and 6) after addition of chymotrypsin. The digestion was performed in TBS containing 1 mM EDTA (lanes 1–3) or 1 mM Ca<sup>2+</sup> (lanes 4–6) at room temperature at 1 mg/mL of  $\gamma$ -module and an enzyme/substrate ratio equal to 1/100 (by mass). Panels B and C show, respectively,  $\gamma$ -module and the D<sub>1</sub> fragment alone (lanes 1 in each panel),  $\gamma$ -module and D<sub>1</sub> with factor XIII (lanes 2), and  $\gamma$ -module and D<sub>1</sub> with factor XIIIa after 0.5, 1, 2, and 3 h of incubation (lanes 3–6). The left lanes in all panels contain molecular mass markers. The cross-linking was performed as described in Materials and Methods. The electrophoretic analysis was performed in 8–25% (panel A and B) and 4–15% (panel C) polyacrylamide gradient gels. The samples containing the D<sub>1</sub> fragment were 2-fold diluted before the analysis.

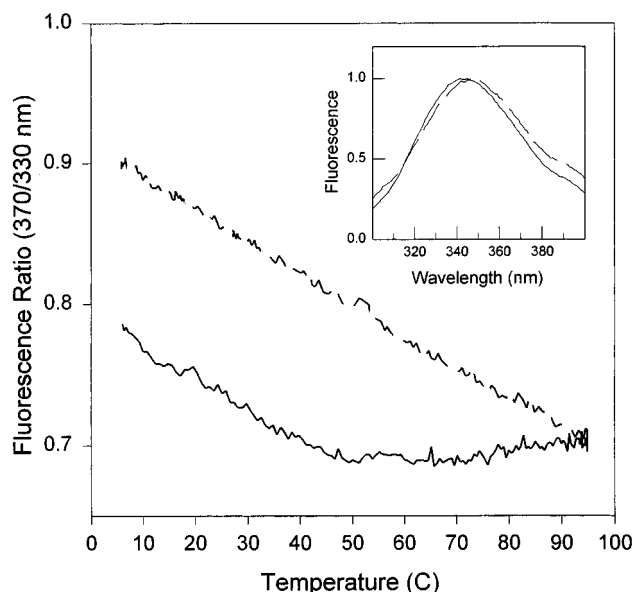


FIGURE 6: Fluorescence-detected denaturation of the 6-kDa NH<sub>2</sub>-terminal fragment of the recombinant  $\gamma$ -module. The fluorescence ratio was registered upon heating (solid line) and cooling (broken line) of the fragment in 20 mM Gly, pH 8.6. The inset shows fluorescence spectra of the fragment before (solid curve) and after (broken curve) heating.

Haverkate & Timan, 1977) and further reinforcing the above conclusion about the Ca<sup>2+</sup>-binding properties of the recombinant protein. Among the fragments in the EDTA-containing digest, the smallest 6-kDa fragment was rather resistant to proteolysis, suggesting that it may represent a compact domain. This fragment was purified to homogeneity in quantity sufficient for sequence analysis and fluorescence study by ion-exchange chromatography of the 60-min digest on a Mono-Q column with subsequent size-exclusion chromatography on Superdex 75. Its NH<sub>2</sub>-terminal sequence was the same as that of the  $\gamma$ -module, indicating that it represents the NH<sub>2</sub>-terminal portion of the latter. The fragment exhibited a fluorescence maximum at 343 nm consistent with the presence of a compact structure with tryptophan partially shielded from solvent (Figure 6, inset). When the fragment was heated while the fluorescence ratio was monitored, the fragment exhibited a denaturation transition that started at

about 50 °C and was not completed at 95 °C (Figure 6); i.e., it occurred in the temperature range higher than the low-temperature transition in the parent  $\gamma$ -module. The fluorescence spectrum was shifted upon denaturation to 348 nm (see inset) and the transition was irreversible since the ratio did not return to the original value upon cooling (dashed line). These results suggest that the high-temperature peak observed in the  $\gamma$ -module by DSC corresponds to the melting of its NH<sub>2</sub>-terminal 6-kDa portion, leaving the rest of the module responsible for the other peak.

**Functional Activity of the  $\gamma$ -Module.** Since reactive Gln398 and Lys406 are normally involved in  $\gamma$ - $\gamma$  cross-linking in fibrin polymers, the recombinant  $\gamma$ -module might be expected to undergo factor XIIIa-catalyzed cross-linking if these residues are properly exposed. As shown in Figure 5B, SDS-PAGE of the  $\gamma$ -module that had been incubated with factor XIIIa revealed the accumulation of dimers; a weak band corresponding to trimers also appeared. Similar results were obtained with the D<sub>1</sub> fragment (Figure 5C), indicating that the efficiency of cross-linking is similar in the two species. Thus the reactive residues in the isolated recombinant  $\gamma$ -module are exposed in the same manner as in the natural fragment.

The major fibrin polymerization site that is complementary to the GPR sequence and has been localized in the C-terminal portion of the  $\gamma$  chain is known to be conformational; i.e., it is not functional in the denatured protein (Cierniewski *et al.*, 1986). Thus one can expect that the  $\gamma$ -module should interfere with fibrin polymerization; i.e., it should exhibit antipolymerization activity as does the natural D<sub>1</sub> fragment, but only if properly folded. We checked the influence of the  $\gamma$ -module on the polymerization process in a standard antipolymerization assay that measures the change in turbidity upon polymerization of fibrin monomer in the presence of different amounts of inhibitor (see Materials and Methods). The results presented in Figure 7 show that the  $\gamma$ -module exhibits a dose-dependent inhibitory effect on the fibrin polymerization process causing a prolongation of the lag time and a sharp decrease in the maximum rate of turbidity growth. The inhibitory effect of the  $\gamma$ -module was about half that of the D<sub>1</sub> fragment. This is probably due to the presence of an additional polymerization site in the  $\beta$ -module

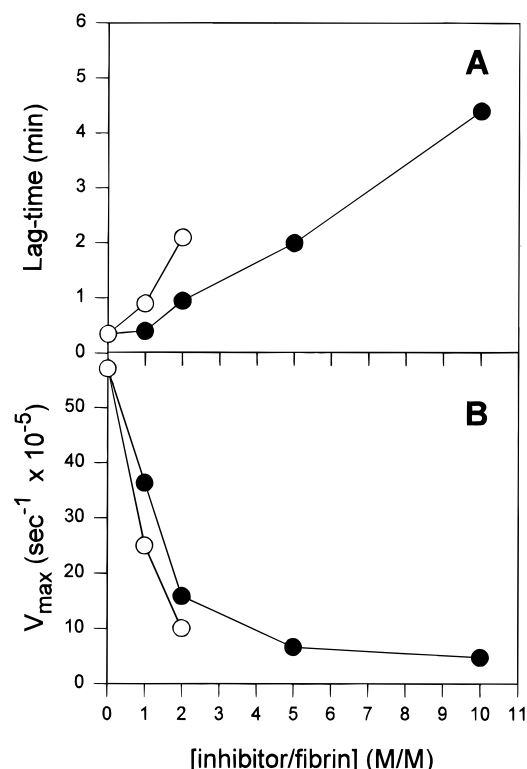


FIGURE 7: Inhibition of fibrin polymerization by the recombinant  $\gamma$ -module (filled circles) and the fibrinogen  $D_1$  fragment (open circles). The delays in polymerization (lag times in panel A) and maximal rates of turbidity growth ( $V_{max}$  in panel B) were determined from the polymerization curves obtained in the presence of different amounts of inhibitors as described in Materials and Methods.

that increases the antipolymerization effect of  $D_1$ . We conclude that those domains in the  $\gamma$ -module that form its polymerization site are folded in a natively like conformation.

It is well-established that fibrinogen supports  $\alpha_{IIb}\beta_3$ -mediated adhesion of platelets and  $\alpha_M\beta_2$ -mediated adhesion of leucocytes via residues  $\gamma 400$ –411 and  $\gamma 190$ –202, respectively (Cheresh *et al.*, 1989; Savage & Ruggeri, 1991; Altieri *et al.*, 1993; Tang *et al.*, 1996). To examine the adhesive functions of recombinant  $\gamma$ -module and to compare them with those of the natural  $\gamma$ -module in the  $D_1$  fragment, we performed adhesion assays with platelets and with the cells that were transfected with  $\alpha_M\beta_2$  receptor. The latter was shown to behave similarly to the naturally occurring one as was reported previously (Zhang & Plow, 1996). As shown in Figure 8A, unstimulated platelets readily attached to the  $\gamma$ -module in a dose-dependent manner. The natural  $D_1$  fragment containing the  $\gamma$ -module behaved similarly. The maximal level of adhesion was similar for both substrates. In parallel experiments, soluble  $\gamma$ -module and  $D_1$  inhibited the adhesion of platelets to immobilized  $\gamma$ -module. At 20  $\mu\text{M}$  (maximal concentration tested) the  $\gamma$ -module was slightly more effective, causing 67% inhibition of adhesion versus 40% for  $D_1$  (not shown). Recombinant  $\gamma$ -module supported the adhesion of  $\alpha_M\beta_2$ -expressing cells more efficiently than  $D_1$  (Figure 8B). The maximal level of adhesion was 3 times higher on  $\gamma$ -module than on  $D_1$ . Moreover, in inhibition experiments, soluble  $\gamma$ -module at 20  $\mu\text{M}$  inhibited cell adhesion by 85%, while  $D_1$  inhibited only by 30% (not shown). For comparison, only 5% of inhibition was achieved by 20  $\mu\text{M}$  synthetic peptide P1 ( $\gamma 190$ –202), whose  $\text{IC}_{50}$  was

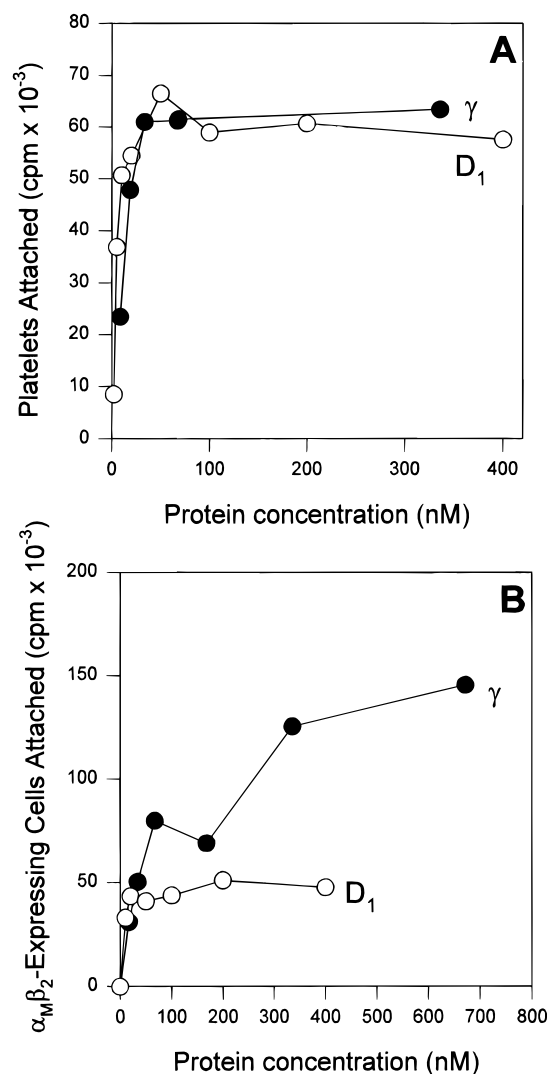


FIGURE 8: Adhesion of unstimulated platelets (A) and  $\alpha_M\beta_2$ -expressing cells (B) to immobilized recombinant  $\gamma$ -module and the  $D_1$  fragment.  $^{51}\text{Cr}$ -labeled platelets and  $\alpha_M\beta_2$ -expressing cells were allowed to attach to wells coated with different concentrations of  $\gamma$ -module (filled circles) or  $D_1$  fragment (open circles) as described in Materials and Methods. The nonadherent cells were removed by washing. The adherent cells were solubilized with SDS and bound  $^{51}\text{Cr}$  was quantitated.

270  $\mu\text{M}$ . Thus, the cell adhesion properties of the recombinant  $\gamma$ -module were fully preserved.

## DISCUSSION

One of the goals of this study was to express the fibrinogen  $\gamma$ -module and to check if its structural integrity and functional properties are preserved in the absence of neighboring domains. The choice of the pET-20b expression vector was based on our previous success with the use of this system to express different variants of the fibrinogen  $\alpha_C$  domain (Matsuka *et al.*, 1996). In addition, a similar pET-11 system was successfully used for the expression of several segments of tenascin, including its fibrinogen-like module that is homologous to the fibrinogen  $\gamma$ -module (Aukhil *et al.*, 1993). When refolding of the  $\gamma$ -module was first performed according to the protocol described for the refolding of the tenascin module (Aukhil *et al.*, 1993), all protein was found in the pellet (results not presented). However, the protocol described here resulted in soluble and functionally active protein. Although only about 20% of the

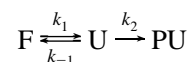
expressed protein was correctly refolded and soluble in TBS, the final yield was still high, about 20–30 mg/L of the bacterial culture.

Since the  $\gamma$ -module was expressed in a bacterial system and was subjected to *in vitro* refolding, it was important to characterize its folding status and stability in comparison to the natural  $\gamma$ -module in fibrinogen or its D fragment. We obtained several lines of evidence for the presence of compact structure in the TBS-soluble fraction of the  $\gamma$ -module. First, its fluorescence spectrum was similar to that of D<sub>1</sub> fragment. Second, the module exhibited a fluorescence-detected sigmoidal transition upon heating in the fluorometer. Third, multiple heat-induced transitions were also detected by DSC. The fluorescence-detected transitions in both the recombinant  $\gamma$ -module and the D fragment were Ca<sup>2+</sup>-dependent, suggesting that the Ca<sup>2+</sup>-binding domain of the former was properly folded. The importance of such a thorough structural characterization is illustrated by the fact that the initial preparation that was soluble at pH  $\geq$  8.0, while exhibiting some properties of a folded protein ( $\lambda_{\text{max}}$  at 343 nm and sigmoidal transition), consisted mainly of soluble noncovalent oligomers by size-exclusion chromatography. Furthermore, it did not exhibit noticeable Ca<sup>2+</sup>-induced stabilization, suggesting that its Ca<sup>2+</sup>-binding domain was not folded properly and that the Ca<sup>2+</sup>-binding site is conformational. Upon dialysis against TBS, ~80% of the material precipitated and the soluble fraction was monomeric and exhibited Ca<sup>2+</sup> binding. All experiments described in this paper were performed with the TBS-soluble fraction.

The temperature-induced denaturation profiles of the  $\gamma$ -module indicated that at least some of the domains are less stable than are the same domains in the natural D fragment, which also contains the  $\beta$ -module and the TSD domain. In addition, the melting of the two thermolabile domains in the  $\gamma$ -module occurred in a less cooperative manner than in the D<sub>1</sub> fragment as evident from a comparison of the sharpness of the low-temperature peaks presented in Figures 3 and 4. This suggests an interaction between the four thermolabile domains in the D<sub>1</sub> fragment and is in agreement with our previous conclusion about stabilizing interactions between domains in the D region of fibrinogen (Medved *et al.*, 1986, 1988; Litvinovich *et al.*, 1995). Nonetheless, the major functional sites of the recombinant  $\gamma$ -module were essentially intact. The module bound Ca<sup>2+</sup> and was stabilized by it against denaturation and proteolysis. Its polymerization site was functionally active, resulting in substantial antipolymerization activity. It was also efficiently cross-linked by factor XIIIa and bound to platelets similarly to the D<sub>1</sub> fragment. The recombinant  $\gamma$ -module also supported the adhesion of  $\alpha_M\beta_2$ -transfected cells and in the fluid phase was almost 3 times more effective than D<sub>1</sub> as an inhibitor of that adhesion. This suggests that the binding site that was localized in the 190–202 region of the  $\gamma$ -module (Altieri *et al.*, 1993) may be partially hidden in the D<sub>1</sub> fragment by interaction with the  $\beta$ -module or TSD. These domain–domain interactions, absent in the recombinant  $\gamma$ -module, may serve to regulate the expression of the  $\alpha_M\beta_2$ -binding site in the natural protein during the fibrinogen-dependent inflammatory response.

Another goal of this study was to define the smallest regions (domains) in the  $\gamma$ -module that would adopt a compact structure and preserve function if expressed independently. For this purpose we performed thermodynamic

analysis of the heat-induced denaturation of the  $\gamma$ -module to establish its domain structure. Although the denaturation of the module was not reversible under the conditions employed, it was still possible to analyze the process and to obtain reasonable data. Indeed, as was shown in multiple studies, protein unfolding is an equilibrium process and irreversibility is caused usually by some secondary phenomenon that prevents or drastically retards the back reaction according to the following scheme:



where F represents the native (folded) state, U represents the reversibly denatured (unfolded) state, and PU represents the irreversibly denatured (postunfolded) state. If  $k_1$  and  $k_{-1}$  are both  $\gg k_2$  and the sample is heated fast enough, the results can be analyzed in terms of equilibrium thermodynamics, even though continued heating at or above the transition temperature may lead to the completion of the postunfolding process and consequent failure to reproduce the given transition in a second scan (Privalov & Potekhin, 1986; Privalov & Medved, 1982; Manly *et al.*, 1985; Edge *et al.*, 1988; Sanchez-Ruiz *et al.*, 1988). In this connection, it can be pointed out that the denaturation of the  $\gamma$ -module is in principle a reversible process since it was easily refolded by dialysis from urea (see Results section) and that a 2-fold decrease in the rate of heating of the  $\gamma$ -module did not significantly affect the position and shape of the endotherm (not shown). In addition, removal of Ca<sup>2+</sup> prevented aggregation even upon heating of the  $\gamma$ -module up to 130 °C and diminished substantially the distortion of the endotherm in the region following the first peak (Figure 3B). These facts strengthen the validity of the deconvolution analysis.

On the basis of the previous study with fibrinogen and its proteolytic fragments, we proposed that the  $\gamma$ -module (residues 148–411) should contain two independently folded thermolabile domains, one in the NH<sub>2</sub>-terminal half and the other in the COOH-terminal half with a border at residues 302–303 (see upper scheme in Figure 1) (Medved *et al.*, 1986; Medved, 1990). The existence of two thermolabile domains was confirmed directly here in the DSC experiments with the recombinant module. At the same time these experiments revealed a new high-temperature transition, reflecting the presence of a thermostable structure that was also found in the  $\gamma$ - and  $\beta$ -modules of the natural D fragment. Although the presence of the high-temperature peak on the endotherm of the  $\gamma$ -module was obvious, we were unable to determine unambiguously how many thermostable domains, one or two, melt in this peak. At this time we can conclude definitely that the  $\gamma$ -module consists of at least three domains, two thermolabile and at least one thermostable. Additional experiments with the 6-kDa proteolytic fragment of the  $\gamma$ -module allowed us to localize one thermostable domain in the NH<sub>2</sub>-terminal portion. Taking into account the size of this fragment, one can assume that this domain is formed by approximately the 148–200 portion of the  $\gamma$  chain, which may include the  $\alpha_M\beta_2$ -binding site, and that the neighboring 200–302 region comprises a separate thermolabile domain. The remaining portion ( $\gamma$ 303–411) contains the other thermolabile domain and possibly an additional thermostable domain. The presence of two domains in this portion would



be consistent with evidence that  $\text{Ca}^{2+}$  binding occurs within a  $\sim 4$ -kDa region beginning at  $\gamma 303$  and ending most probably at  $\gamma 357$  (Nieuwenhuizen & Haverkate, 1983; Henschen & McDonagh, 1986). Taking into account that the D<sub>int</sub> fragment containing this region and lacking the following COOH-terminal 9-kDa portion of  $\gamma$ -chain binds  $\text{Ca}^{2+}$  (Nieuwenhuizen & Haverkate, 1983) and given the notion developed herein that  $\text{Ca}^{2+}$  binding requires proper folding, one can speculate that this region folds independently from the following  $\sim 9$ -kDa region, which would then be available for a fourth domain.

In summary, detailed structural analysis of the recombinant fibrinogen  $\gamma$ -module confirmed its structural integrity and revealed the presence of at least one thermostable domain in addition to the two thermolabile domains characterized earlier. The results bring the number of the independently folded domains in fibrinogen to at least 18, two  $\alpha\text{C}$  domains (Medved *et al.*, 1983), two domains in the central region (Privalov & Medved, 1982), and at least seven in each of the two D regions (this study). Functional analysis revealed that all binding sites of the  $\gamma$ -module are preserved in the absence of the neighboring domains that stabilize its structure in fibrinogen. Moreover, the Mac-1 binding site was found to be more active in the  $\gamma$ -module than in D<sub>1</sub>, suggesting a possible role for domain-domain interactions in regulating the activity of the fibrinogen D region.

#### NOTE ADDED IN PROOF

While this paper was in press, a three-dimensional structure of a similar recombinant  $\gamma$ -module was reported by Yee *et al.* (1997). The structure reveals three domains in agreement with our conclusion. Furthermore, their third domain (domain C) appears to comprise two lobes which could ultimately prove to be independently folded as speculated in the present paper.

#### ACKNOWLEDGMENT

We thank Dr. S. Lord for provision of full-length cDNA encoding the fibrinogen  $\gamma$  chain, Dr. L. Zhang for providing the  $\alpha\text{M}\beta_2$ -transfected 293 cells, and Dr. E. Plow for helpful discussion.

#### REFERENCES

- Altieri, D. C., Plescia, J., & Plow, E. F. (1993) *J. Biol. Chem.* 268, 1847–1853.
- Aukhil, I., Joshi, P., Yan, Y., & Erickson, H. P. (1993) *J. Biol. Chem.* 268, 2542–2553.
- Bishop, P. D., Teller, D. C., Smith, R. A., Lasser, G. W., Gilbert, T., & Seale, R. L. (1990) *Biochemistry* 29, 1861–1869.
- Bolyard, M. G., & Lord, S. T. (1988) *Gene* 66, 183–192.
- Cheresh, D. A., Berliner, S. A., Vincente, V., & Ruggeri, Z. M. (1989) *Cell* 58, 945–953.
- Cierniewski, C. S., Kloczewiak, M., & Budzynski, A. Z. (1986) *J. Biol. Chem.* 261, 9116–9121.
- Doolittle, R. F. (1984) *Annu. Rev. Biochem.* 53, 195–229.
- Doolittle, R. F. (1992) *Protein Sci.* 1, 1563–1577.
- Doolittle, R. F. (1994) in *The molecular basis of blood diseases* (Stamatoyannopoulos, G., Nienhuis, A. W., Majerus, P. W., & Varmus, H., Eds.) pp 701–723, W. B. Saunders Co., Philadelphia, PA.
- Edelhoc, H. (1967) *Biochemistry* 6, 1948–1954.
- Edge, E., Allewell, N. M., & Sturtevant, J. M. (1988) *Biochemistry* 27, 8081–8087.
- Filimonov, V. V., Potekhin, S. A., Matveev, S. V., & Privalov, P. L. (1982) *Mol. Biol. (Mosk.)* 16, 551–562.
- Gill, S. C., & von Hippel, P. H. (1989) *Anal. Biochem.* 182, 319–326.
- Gorkun, O. V., Veklich, Y. I., Medved, L. V., Henschen, A. H., & Weisel, J. W. (1994) *Biochemistry* 33, 6986–6997.
- Haverkate, F., & Timan, G. (1977) *Thromb. Res.* 10, 803–812.
- Hawiger, J., Kloczewiak, M., & Timmons, S. (1983) *Ann. N.Y. Acad. Sci.* 408, 521–535.
- Henschen, A., & McDonagh, J. (1986) in *Blood Coagulation* (Zwaal, R. F. A., & Hemker, H. C., Eds.) pp 171–241, Elsevier Science Publishers, Amsterdam.
- Litvinovich, S. V., Henschen, A. H., Krieglstein, K. G., Ingham, K. C., & Medved, L. V. (1995) *Eur. J. Biochem.* 229, 605–614.
- Manly, S. P., Matthews, K. S., & Sturtevant, J. M. (1985) *Biochemistry* 24, 3842–3846.
- Matsuka, Y. V., Medved, L. V., Migliorini, M. M., & Ingham, K. C. (1996) *Biochemistry* 35, 5810–5816.
- Medved, L. V. (1990) *Blood Coagul. Fibrinolysis* 1, 439–442.
- Medved, L. V., Privalov, P. L., & Ugarova, T. P. (1982) *FEBS Lett.* 146, 339–342.
- Medved, L. V., Gorkun, O. V., & Privalov, P. L. (1983) *FEBS Lett.* 160, 291–295.
- Medved, L. V., Gorkun, O. V., Manyakov, V. F., & Belitsker, V. A. (1985) *FEBS Lett.* 181, 109–112.
- Medved, L. V., Litvinovich, S. V., & Privalov, P. L. (1986) *FEBS Lett.* 202, 298–302.
- Medved, L. V., Platonova, T. N., Litvinovich, S. V., & Likinova, N. I. (1988) *FEBS Lett.* 232, 56–60.
- Nieuwenhuizen, W., & Haverkate, F. (1983) *Ann. N.Y. Acad. Sci.* 408, 92–96.
- Niewiarowski, S., Kornecki, E., Budzynski, A. Z., Morinelli, T. A., & Tuszynski, G. P. (1983) *Ann. N.Y. Acad. Sci.* 408, 536–555.
- Privalov, P. L., & Medved, L. V. (1982) *J. Mol. Biol.* 159, 665–683.
- Privalov, P. L., & Potekhin, S. A. (1986) *Methods Enzymol.* 131, 4–51.
- Sanchez-Ruiz, J. M., Lopez-Lacomba, J. L., Cortijo, M., & Mateo, P. L. (1988) *Biochemistry* 27, 1648–1652.
- Savage, B., & Ruggeri, Z. M. (1991) *J. Biol. Chem.* 266, 11227–11233.
- Studier, F. W., Rosenberg, A. H., Dunn, J. J., & Dubendorff, J. W. (1995) *Methods Enzymol.* 185, 60–89.
- Tang, L., Ugarova, T. P., Plow, E. F., & Eaton, J. W. (1996) *J. Clin. Invest.* 97, 1329–1334.
- Tran, H., Tanaka, A., Litvinovich, S. V., Medved, L. V., Haudenschild, C. C., & Argraves, W. S. (1995) *J. Biol. Chem.* 270, 19458–19464.
- Yee, V. C., Pratt, K. P., Cote, H. C. F., Le Trong, I., Chung, D. W., Davie, E. W., Stenkamp, R. E., & Teller, D. C. (1997) *Structure* 5, 125–138.
- Yonekawa, O., Voskuilen, M., & Nieuwenhuizen, W. (1992) *Biochem. J.* 283, 187–191.
- Zhang, L., & Plow, E. F. (1996) *J. Biol. Chem.* 271, 18211–18216.

BI962795L